Clim Dyn (2010) 34:859–872
DOI 10.1007/s00382-009-0564-1

# Using a global climate model to evaluate the influences of water vapor, snow cover and atmospheric aerosol on warming in the Tibetan Plateau during the twenty-first century

**Imtiaz Rangwala · James R. Miller · Gary L. Russell · Ming Xu**

Received: 2 October 2008 / Accepted: 23 March 2009 / Published online: 8 April 2009


**Abstract** We examine trends in climate variables and their interrelationships over the Tibetan Plateau using global climate model simulations to elucidate the mechanisms for the pattern of warming observed over the plateau during the latter half of the twentieth century and to investigate the warming trend during the twenty-first century under the SRES A1B scenario. Our analysis suggests a 4°C warming over the plateau between 1950 and 2100. The largest warming rates occur during winter and spring. For the 1961–2000 period, the simulated warming is similar to the observed trend over the plateau. Moreover, the largest warming occurs at the highest elevation sites between 1950 and 2100. We find that increases in (1) downward longwave radiation (DLR) influenced by increases in surface specific humidity ($q$), and (2) absorbed solar radiation (ASR) influenced by decreases in snow cover extent are, in part, the reason for a large warming trend over the plateau, particularly during winter and spring. Furthermore, elevation-based increases in DLR (influenced by $q$) and ASR (influenced by snow cover and atmospheric aerosols) appear to affect the elevation dependent warming trend simulated in the model.

**Keywords** Climate change · High elevation · Tibetan Plateau · Global climate model · Specific humidity · Downward longwave

I. Rangwala (✉)
Department of Environmental Sciences, Rutgers University, 14 College Farm Road, New Brunswick, NJ 08901, USA
e-mail: imtiazr@envsci.rutgers.edu

J. R. Miller
Institute of Marine and Coastal Sciences, Rutgers University, New Brunswick, USA

G. L. Russell
NASA Goddard Institute for Space Studies, New York, USA

M. Xu
Institute of Geographic Sciences and Natural Resources Research, Chinese Academy of Sciences, Beijing, People's Republic of China

M. Xu
Department of Ecology, Evolution and Natural Resources, Rutgers University, New Brunswick, USA

## 1 Introduction

There has been much interest recently in examining the nature of climate change in the Tibetan Plateau during the late twentieth century. It is understood that this region may be among the most sensitive to global climate change (Du et al. 2004; Liu and Chen 2000). However, observations are not spatially uniform over the plateau. Most of the climate data is available from weather stations located in the eastern half of the plateau which is more inhabited and where the average altitude is relatively lower.

The analyses of these climate data have shown that the Tibetan Plateau has warmed very rapidly (0.2–0.4°C/decade) in the latter half of the twentieth century (Du et al. 2004; Liu and Chen 2000; Niu et al. 2004; Rangwala et al. 2009; Xu et al. 2007). This warming trend has been largest during the winter months; fall has the next highest warming rate, while summer and spring show relatively less warming (Du et al. 2004; Liu and Chen 2000; Chen et al. 2006; You et al. 2007). Liu and Chen (2000) estimated that the winter warming has been twice as large as the annual mean. However, comparisons between winter and annual warming rates vary significantly among other studies based on the selection of station and the observation period

(Du et al. 2004; Chen et al. 2006; You et al. 2007). Moreover between 1991 and 2000, Rangwala et al. (2009) found that spring and summer months appeared to have warmed rapidly over the plateau.

Furthermore, Liu and Chen (2000) suggested a pattern of elevation dependent warming (EDW) over the plateau between 1961 and 1990 from a trend analysis of 178 weather stations. We also found a comparable trend of EDW in our analysis for the 1961–1990 period, however the trend becomes weaker when we consider the 1961–2000 period (Rangwala et al. 2009). Regarding the trends for the temperature extremes in the plateau, You et al. (2008) did not find any strong correlation with elevation between 1961 and 2005.

In this study, we examine the output from two simulations of a global climate model to (a) compare the modeled and observed patterns of climate change over the plateau in the latter half of the twentieth century, (b) examine potential changes through the twenty-first century and (c) elucidate the mechanisms for these climatic changes. Details of the model and the observations are provided in Sect. 2. Section 3 provides an analysis of the observations and the modeled results. Possible influences of changes in low level water vapor and snow cover extent on the pattern of warming in the plateau are described in Sects. 4 and 5, respectively. Section 6 examines the mechanisms for an EDW over the plateau and Sect. 7 provides concluding remarks.

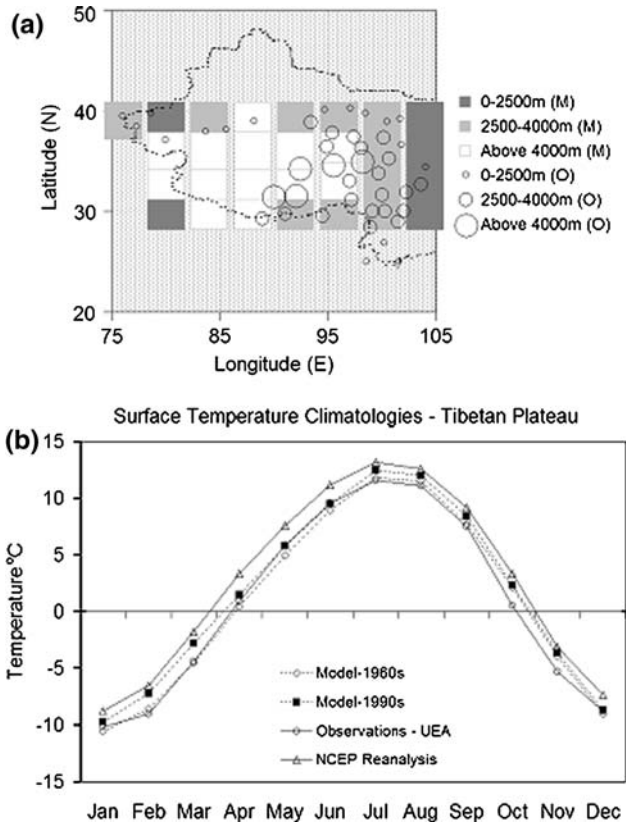


**Fig. 1** **a** Location and elevation range of model grids (M; *squares*) and observation stations (O; *circles*) used to study the Tibetan Plateau region. The *dashed curve* demarks the political boundary of China. **b** Comparison of surface temperature climatologies over the Tibetan Plateau: modeled (1960s and 1990s) versus observed (University of East Anglia, UEA, 1961–1990; National Center for Environmental Prediction (NCEP) reanalysis, 1982–1994)

## 2 Description of observations and the global climate model

Observations of climate variables such as surface air temperature, surface specific humidity ($q$), cloud cover and precipitation from 1961 to 2000 are obtained from the dataset described in Xu et al. (2006). For this study, the Tibetan Plateau region lies between 80–108°E and 27–39°N (see Fig. 1a). There were 43 observation stations identified over the plateau, and most of them are located on the eastern side of the plateau where the average elevation is relatively lower. Our study region is extended eastward from the typical plateau region to obtain adequate observation stations in order to validate the model's performance for the whole region. Moreover, owing to the sparsity of observation stations in the western half of the plateau, our analysis of the trends there is less reliable.

Simulated trends in the selected climate variables over the Tibetan Plateau are obtained from the GISS-AOM (Goddard Institute for Space Studies-Atmosphere Ocean Model, NASA) global climate model, based on Russell et al. (1995; http://aom.giss.nasa.gov). The analysis presented in this paper is based on the output from two model experiments—SRES A1B and control. The two model experiments are identical except that the SRES A1B simulation uses observed greenhouse gases and estimated spatial distributions of atmospheric sulfate burden from Boucher and Pham (2002) for the 1850–2000 period. For the twenty-first century, greenhouse gases are observed up to year 2003 followed by IPCC SRES A1B (Houghton et al. 2001); the sulfate burden is from SRES A1B (Pham et al. 2005). For the control simulation, the atmospheric composition is fixed at 1850 values between 1850 and 2100. All anomalies presented here are differences between the A1B and the control simulations.

The plateau region considered in the model simulations has 29 grid cells, which are located between 80–108°E and 27–39°N. The horizontal resolution is $3 \times 4°$ in latitude and longitude, respectively. The atmospheric column for each grid cell has 12 layers. The lowest layer is 400 kg/m$^2$ or approximately 39 mb thick; higher layers are variable in thickness depending on the location. To extract the elevation dependent climate trends in the plateau, we organized

the model output into three different elevation regions: 0–2,500 m, 2,500–4,000 m, and 4,000–5,300 m. There are respectively 6, 10 and 13 grid cells associated with these regions. Table 1 shows mean and variability in elevation associated with each grid cell.

Owing to its relatively coarse resolution, the model cannot resolve the effects of high topographic relief at local scales. However, we expect that the large spatial scale of the study region and the large range in mean elevation of the grid cells are sufficient for analysis of the temperature differences in this study. To confirm this, Fig. 1b shows a comparison of the modeled and observed surface temperature climatologies over the study region. The latter include climatologies obtained from New et al. (1999; http://www.cru.uea.ac.uk/) and NCEP reanalysis (http://www.cdc.noaa.gov/cdc/data.ncep.reanalysis.derived.html). We find that the model simulates the observed temperature climatologies on a seasonal basis.

**Table 1** Means and standard deviations for surface elevation (m) for each grid cell

| Grid # | Longitudes (E) | Latitudes (N) | Mean elevation (m) | SD (m) |
|---|---|---|---|---|
| 1 | 76–80 | 36–39 | 2,572 | 1,417 |
| 2 | 80–84 | 36–39 | 1,864 | 897 |
| 3 | 80–84 | 33–36 | 5,146 | 343 |
| 4 | 80–84 | 30–33 | 5,009 | 449 |
| 5 | 80–84 | 27–30 | 1,698 | 1,691 |
| 6 | 84–88 | 36–39 | 3,170 | 1,630 |
| 7 | 84–88 | 33–36 | 5,062 | 193 |
| 8 | 84–88 | 30–33 | 4,994 | 312 |
| 9 | 84–88 | 27–30 | 3,765 | 1,775 |
| 10 | 88–92 | 36–39 | 4,034 | 799 |
| 11 | 88–92 | 33–36 | 5,049 | 191 |
| 12 | 88–92 | 30–33 | 4,900 | 265 |
| 13 | 88–92 | 27–30 | 4,243 | 1,054 |
| 14 | 92–96 | 36–39 | 3,199 | 565 |
| 15 | 92–96 | 33–36 | 4,680 | 230 |
| 16 | 92–96 | 30–33 | 4,797 | 400 |
| 17 | 92–96 | 27–30 | 2,765 | 1,773 |
| 18 | 96–100 | 36–39 | 3,708 | 600 |
| 19 | 96–100 | 33–36 | 4,410 | 261 |
| 20 | 96–100 | 30–33 | 4,415 | 395 |
| 21 | 96–100 | 27–30 | 3,342 | 1,242 |
| 22 | 100–104 | 36–39 | 2,570 | 833 |
| 23 | 100–104 | 33–36 | 3,503 | 573 |
| 24 | 100–104 | 30–33 | 3,524 | 952 |
| 25 | 100–104 | 27–30 | 2,768 | 1,156 |
| 26 | 104–108 | 36–39 | 1,528 | 247 |
| 27 | 104–108 | 33–36 | 1,704 | 554 |
| 28 | 104–108 | 30–33 | 782 | 464 |
| 29 | 104–108 | 27–30 | 852 | 447 |

The initial state of these simulations was based on a 200 year spin-up simulation of initial ocean conditions as described in Levitus et al. (1994). The output from the model experiment is analyzed for the surface energy balance over the plateau between 1950 and 2100. Components of the surface energy fluxes analyzed include downward longwave radiation (DLR), absorbed solar radiation (ASR), upward longwave radiation (ULR), latent heat and sensible heat fluxes.

## 3 Simulated climatic changes over the Tibetan Plateau between 1950 and 2100

Figure 2a shows that the plateau region warmed by 4°C over the entire period of the simulation, 1850–2100. Most of this warming occurred after 1950 and the largest rate of warming (0.52°C/decade) occurred between 2020 and 2060 at all elevations. For the 1961–2000 period, the modeled surface warming rate (0.25°C/decade) is in agreement with the reported observed trends of 0.21°C/decade (Niu et al. 2004) and 0.24°C/decade (Rangwala et al. 2009). The observed warming trend in the plateau is greater than the late twentieth century warming trend of 0.19°C/decade reported for Mainland China by Liu et al. (2004) and 0.12°C/decade in the model simulation (Rangwala et al. 2006).

Moreover, the model experiment demonstrates an EDW trend over the Tibetan Plateau between 1951 and 2100. Figure 2a shows increases in surface temperatures of 5, 4 and 3.5°C between 1950 and 2100 from the highest to the lowest elevation ranges, respectively. The EDW trend becomes larger in the latter half of the twenty-first century. For the 1961–1990 period, the model demonstrates an EDW of 0.037°C/decade/1,000 m over the plateau which is smaller than the observed trend of 0.054°C/decade/1,000 m reported by Liu and Chen (2000) as shown in Fig. 2b. During the twenty-first century, the EDW trend is similar to the late twentieth century trend in the model. However, there is almost a doubling of the warming rate at all elevations during the twenty-first century relative to the rate during the late twentieth century (Fig. 2b).

Figure 3a–b show the spatial patterns of linear trends in observed and modeled temperatures over the plateau in the latter half of the twentieth and twenty-first centuries. Figure 3a exposes the scarcity of observations on the western side of the plateau, where both the mean elevation and the model's warming rate are higher during the late twentieth and the twenty-first century. Therefore, the mean observed warming rate of 0.24°C/decade estimated for the plateau region between 1961 and 2000 might be a conservative estimate.

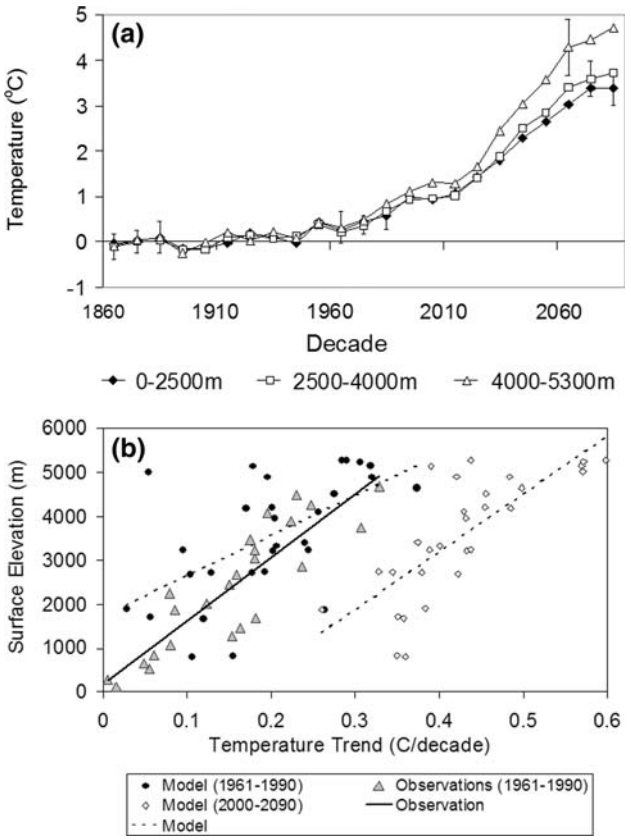


**Fig. 2** **a** Decadally averaged anomalies in surface temperature simulated over the Tibetan Plateau from 1851 to 2100 at three different elevation ranges. Randomly placed *errors bars* for each elevation range are +/−1 standard deviations. **b** Observed (1961–1990; from Liu and Chen 2000) and modeled (1961–1990 and 2000–2090) trends in surface temperature (°C/decade) in the Tibetan Plateau as related to the elevation of the observing station and the model grid, respectively

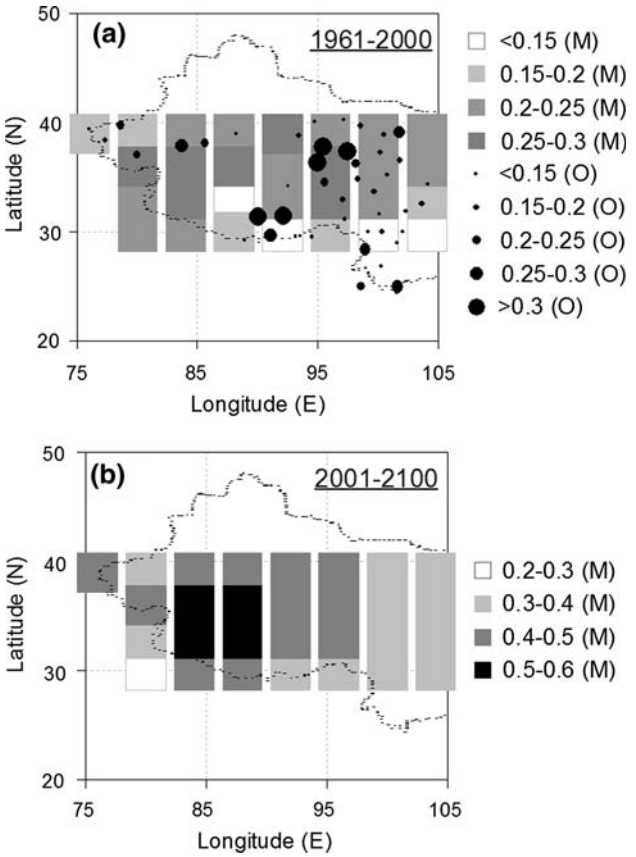


**Fig. 3** **a** Observed and modeled trends in temperature (°C/decade) over the Tibetan Plateau between 1961 and 2000. **b** Modeled temperature trends (°C/decade) between 2001 and 2100

For the twenty-first century, the model projects the largest warming during winter and spring months at higher elevations (Fig. 4a). Warming during these months started earlier in comparison to summer and fall. Even the lower elevation regions below 2,500 m show a similar seasonal contribution to the warming trend in the model, however the differences among the seasonal contributions to the total warming are smaller. Moreover, Fig. 4a shows that the EDW for the twenty-first century is significantly greater during winter and spring than it is in summer and fall.

Figure 4b shows the modeled change in surface energy budgets during the twenty-first century. There are large increases in DLR and ULR at all elevations and all seasons. However during winter, the increases in DLR are larger than ULR particularly at 4,000–5,300 m. During spring and summer, there are large increases in ASR at 4,000–5,300 m and 2,500–4,000 m. At 0–2,500 m, there are large increases in latent heat fluxes and decreases in sensible heat fluxes during all seasons except spring. There is negligible change in sensible heat fluxes at higher elevations; however latent heat fluxes show large increases during winter and spring at 2,500–4,000 m and during summer at 4,000–5,300 m. Moreover, the surface energy fluxes described in Fig. 4b do not completely balance each other, particularly at 4,000–5,300 m. These imbalances occur, in part, because there are large decreases in ice mass owing to melting at 4,000–5,300 m during the twenty-first century. The decreases in surface ice mass and associated runoff are largest during spring and summer.

In concurrence with elevation dependent increases in temperature (Fig. 5a) over the plateau between 1950 and 2100, Fig. 5b shows an elevation-based decrease in snow cover, whereas Fig. 5d–g show that there are elevation-based increases in surface vapor pressure, ASR, DLR and latent heat fluxes. For cloud cover, there is a small decreasing trend except at 4,000–5,300 m (Fig. 5c). In the SRES A1B scenario, the atmospheric sulfate burden is anticipated to increase between 1950 and 2030 and show a decreasing trend for the rest of the twenty-first century (Fig. 5h). The largest increases in sulfate burden occur at the lowest elevations, where the sulfate concentrations are

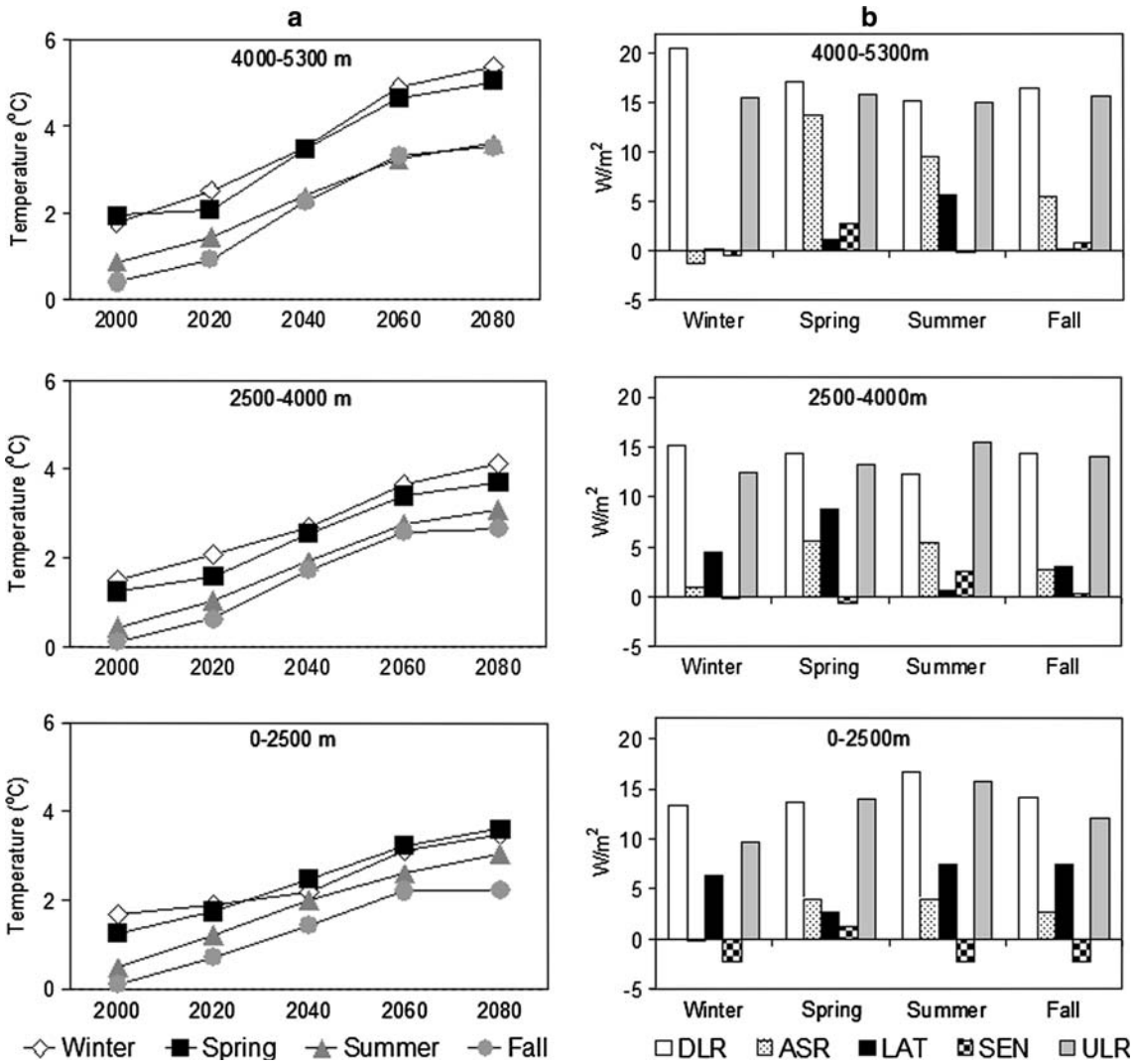


**Fig. 4** **a** Modeled anomalies in the seasonal surface temperature between 2000 and 2090, and **b** changes in surface energy fluxes between two decades—"2081–2090" minus "2001–2010"—over the Tibetan Plateau at three different elevation ranges. Surface energy fluxes plotted, in order, are *DLR* (downward longwave radiation), *ASR* (absorbed solar radiation), *LAT* (latent heat fluxes), *SEN* (sensible heat fluxes), and *ULR* (upward longwave radiation)

more than three times greater than at the highest elevations between 1980 and 2040.

## 4 Effect of surface water vapor on winter warming

Both the observations and model demonstrate a prominent winter warming over the plateau for the 1961–2000 period. The model simulation projects this warming to continue during the twenty-first century (Fig. 4a). Evaluation of surface energy fluxes suggests that greater increases in DLR, relative to ULR, during the winter months at all elevations are, in large part, associated with a greater warming of the plateau during winter (Fig. 4b).

Figure 5d and f show that the modeled changes in DLR correspond to changes in surface vapor pressure. Partial correlation calculations suggest that vapor pressure is positively correlated ($r = 0.5$–$0.7$) to DLR at all elevations, though not as strongly as surface temperature is to DLR ($r > 0.85$). Because of the distribution of lines of absorption and emission of thermal radiation by water vapor, DLR is roughly proportional to the logarithm of surface humidity. Thus, changes in specific humidity ($q$) have a greater effect on DLR in cold seasons and at higher elevations where the initial $q$ is smaller. Ruckstuhl et al. (2007) present observational evidence from the Alps to support this conclusion. They suggest an enhancement in the absorption of outgoing longwave radiation in the

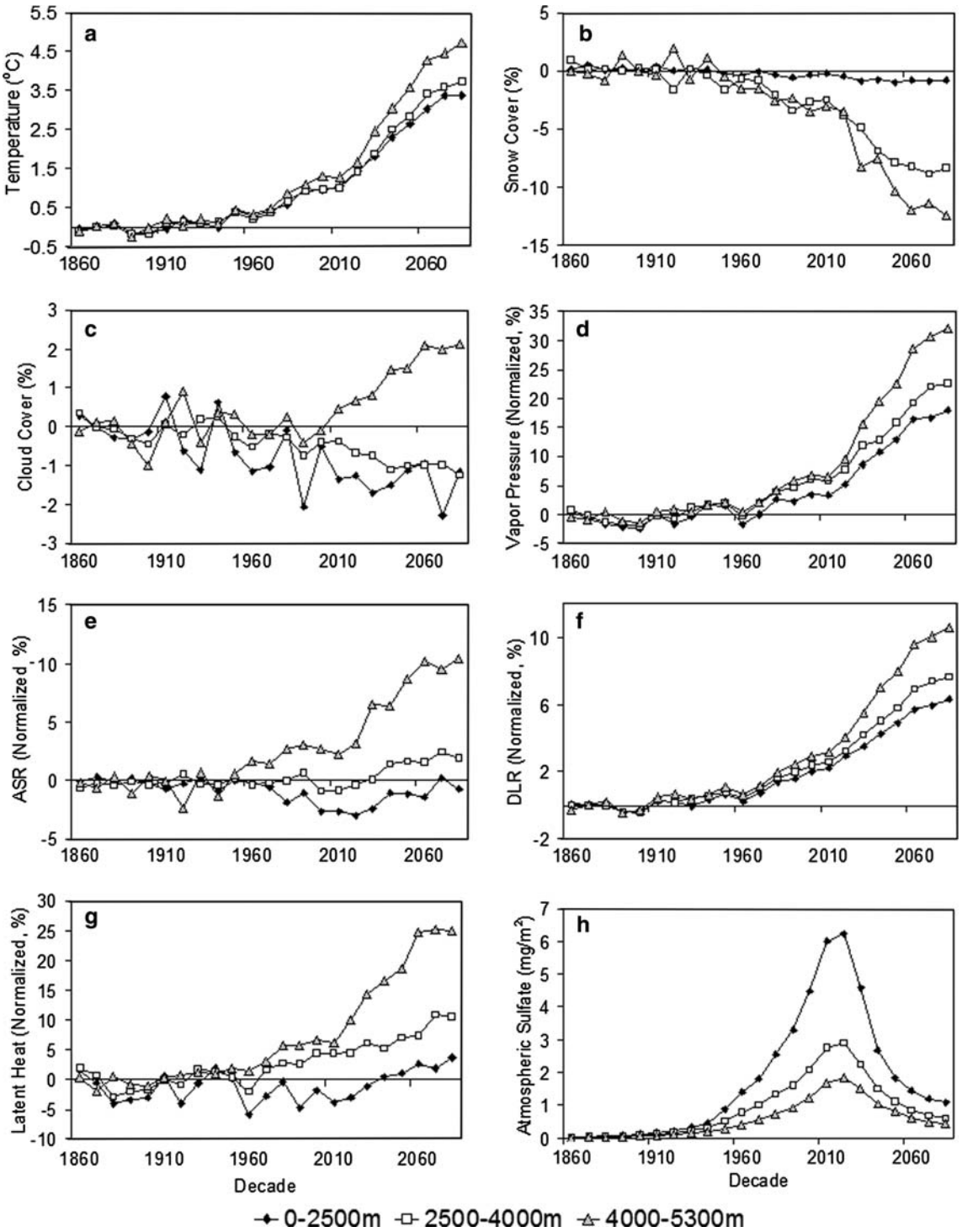


**Fig. 5** Decadally averaged anomalies in the modeled climate variables—**a** temperature (°C), same as Fig. 2a, **b** snow cover (%), **c** cloud cover (%), **d** vapor pressure (normalized, %), **e** ASR (normalized, %), **f** DLR (normalized, %), **g** surface latent heat fluxes (normalized, %) and **h** atmospheric sulfate burden (mg/m$^2$) based on Boucher and Pham (2002) and Pham et al. (2005)—over the Tibetan Plateau between 1951 and 2100 at three different elevations. The normalized variables have been normalized by the mean of the control run during the twentieth century

atmospheric window (8–13 μm) at higher elevations where the average atmospheric vapor concentrations are lower. We expect this absorption gain to be greatest during the winter months when the atmospheric water vapor content is lowest over the plateau (Rangwala et al. 2009).

Figure 6 shows the modeled relationship between DLR and $q$ for each season and elevation range. A slope at any location on the curve describes the sensitivity ($\lambda$) of DLR to $q$. As $q$ becomes smaller, the slope, and hence the sensitivity of DLR to changes in $q$ becomes larger (Table 2). The power law relationships described in the figure suggest that significantly large changes occur in DLR owing to changes in $q$ when the latter is less than 2.5 g/kg. The model's power law relationship, obtained using all the data points shown in the figure, is comparable to the power law relationship of Ruckstuhl et al. (2007) for all sky conditions in the Swiss Alps. The model's power law does better in capturing the relationship between DLR and $q$ at higher elevations (2,500–5,300 m), whereas the power law from Ruckstuhl et al. (2007) does better at 0–2,500 m. The model shows a slightly higher sensitivity of DLR to $q$ as compared to the sensitivity from the power law relationship of Ruckstuhl et al. (2007) when $q$ is higher than 0.7 g/kg which is true at all elevations and seasons in the plateau (Table 2). As an example, the model sensitivity is 1.6% higher during winter at 4,000–5,300 m, where the average observed $q$ is 1.1 g/kg between 1961 and 2000.

Modeled increases in DLR over the plateau appear to be primarily associated with increases in $q$ between 1950 and 2100 (Fig. 7). The changes in DLR and $q$ are strongly correlated, particularly, at the highest elevation ($r > 0.99$). Furthermore, Fig. 7 shows that smaller increases in $q$ at 4,000–5,300 m are associated with large increases in DLR during the cold season (winter, early spring and late fall). Changes in the modeled cloud cover are small and not correlated with changes in DLR over the plateau, except during winter at 4,000–5,300 m (Fig. 8). However, even for the latter case, only the partial correlation of DLR to $q$ is significant. Moreover, the observed cloud cover is decreasing between 1961 and 2000 except at the lowest elevations (Fig. 5c); the largest decreases are at 4,000–5,300 m during winter and summer months. Duan and Wu (2006) suggest increases in the observed low level nocturnal cloud cover over the plateau between 1961 and 2003, even though the total cloud cover is decreasing during this period. However, there does not appear to be any apparent elevation dependence to this phenomenon in their analysis.

Rangwala et al. (2009) calculated seasonal increases in DLR over the Tibetan Plateau resulting from the observed increases in $q$ for the 1961–2000 period based on the sensitivity obtained from the power law relationship of Ruckstuhl et al. (2007) shown in Fig. 6. Large increases in DLR are found to be associated with observed $q$ trends between 1961 and 2000 during cold seasons particularly at higher elevations. For the twenty-first century, further warming of the atmosphere under the continuing greenhouse gas forcing will increase the atmospheric water vapor content. During cold seasons in the twenty-first century, $q$ is expected to stay in the range that has large sensitivities to DLR, and we expect large increments in the absorption and re-emission of longwave radiation in the surface boundary layer. Therefore, for most of the twenty-first century, we project a large warming trend in winter at high elevation due to increases in the surface water vapor over the plateau.

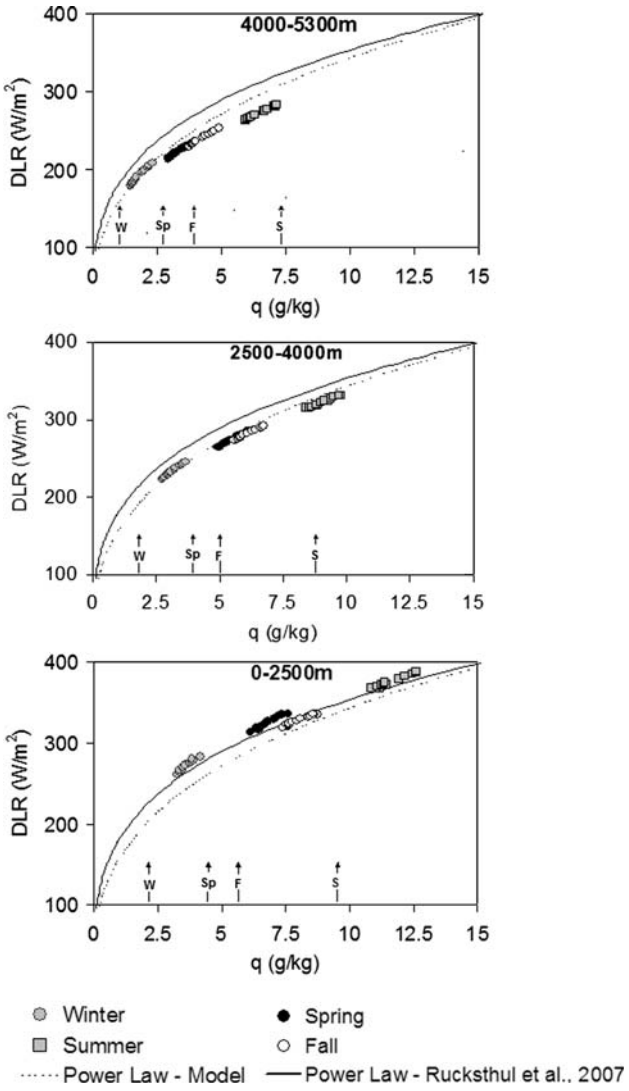


**Fig. 6** Seasonally resolved modeled relationship between DLR and $q$ for three different elevation regions in the Tibetan Plateau. Each point is a decadally averaged value for the period between 1950 and 2100. For each season, the points move upward and to the right with time. The power law curves are DLR $= 181.4 \times q^{0.29}$ (Ruckstuhl et al. 2007) and DLR $= 156.6 \times q^{0.34}$ (model). The *arrows* indicate the location of mean values of observed $q$ over the plateau for the 1961–2000 period during winter (W), spring (Sp), summer (S) and fall (F)

**Table 2** Comparison of sensitivities ($\lambda$) of DLR to $q$ between relationships obtained from the model and Ruckstuhl et al. (2007) at different elevations in the Tibetan Plateau. $\lambda$ (W m$^{-2}$ kg g$^{-1}$) measurements are based on the average values of $q$ (g kg$^{-1}$) between 1961 and 2000

| Elevation | 4,000–5,300 m | | 2,500–4,000 m | | 0–2,500 m | |
|---|---|---|---|---|---|---|
| | $\lambda$ (model) | $\lambda$ (Rucksthul et al.) | $\lambda$ (model) | $\lambda$ (Rucksthul et al.) | $\lambda$ (model) | $\lambda$ (Rucksthul et al.) |
| Winter | 50.5 | 49.7 | 38.1 | 36.7 | 32.3 | 30.7 |
| Spring | 27.2 | 25.5 | 21.8 | 20.2 | 19.9 | 18.3 |
| Summer | 14.4 | 12.9 | 12.8 | 11.3 | 12.0 | 10.6 |
| Fall | 22.2 | 20.5 | 18.8 | 17.1 | 17.5 | 15.9 |

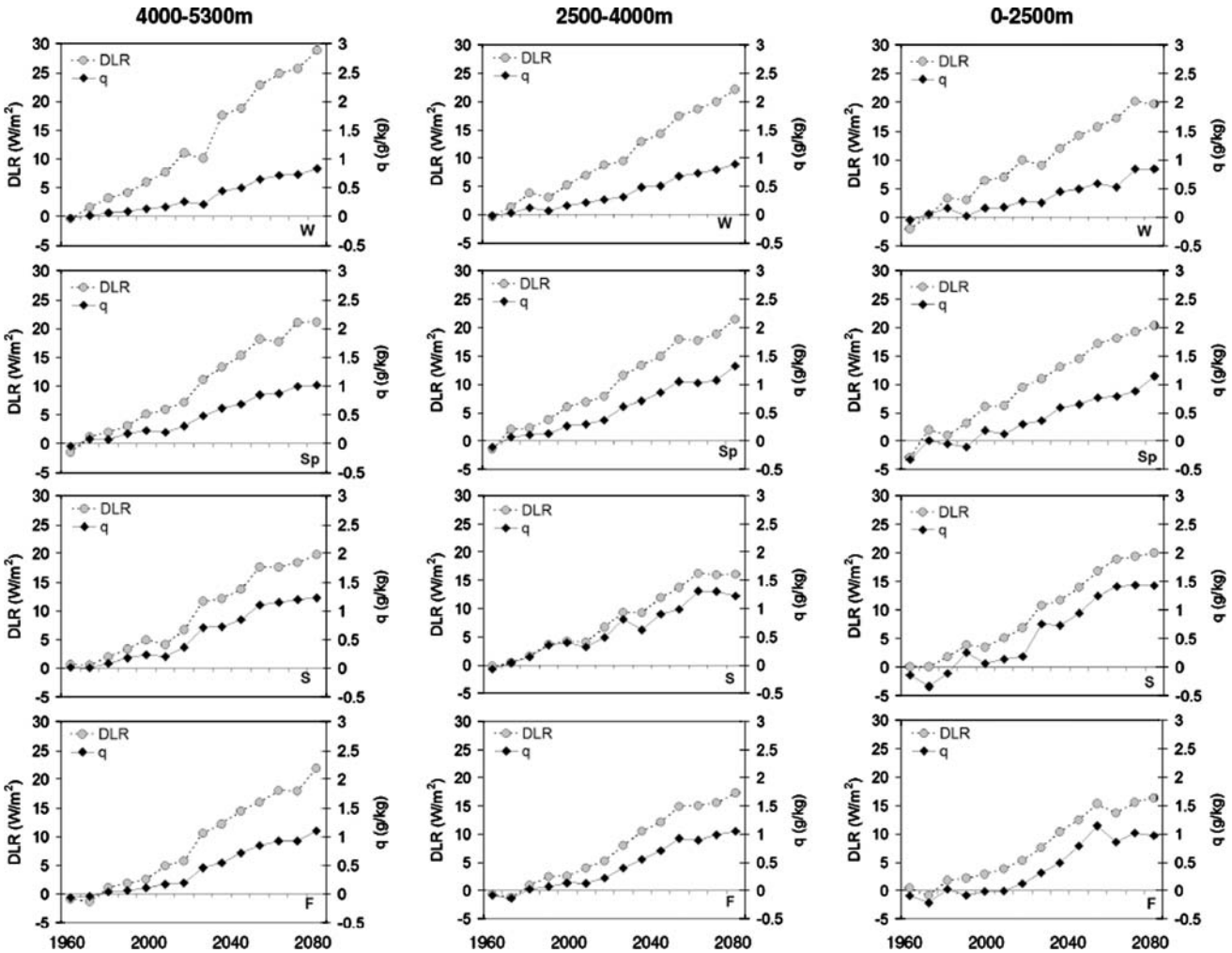


**Fig. 7** Seasonal changes in decadal means with respect to 1950s in DLR (W/m$^2$; *left axis*) and $q$ (g/kg; *right axis*) for each decade between 1960s and 2090s at the three elevation regions in the Tibetan Plateau

## 5 Effect of snow cover extent on warming in spring and fall

During fall, the model shows less warming on the plateau than spring (Fig. 4a). For both model and observations, the atmospheric water vapor content in the fall is slightly higher than in the spring. Observations show similar increases in $q$ for spring and fall between 1961 and 2000 (Rangwala et al. 2009). Considering similar sensitivities of DLR to $q$ during both spring and fall, the water vapor influences on DLR during fall are not significant enough to cause the larger observed warming of the surface in fall relative to spring.

We find that the observed increases in the maximum temperature at all elevations during fall are much larger than during spring between 1961 and 2000; the minimum

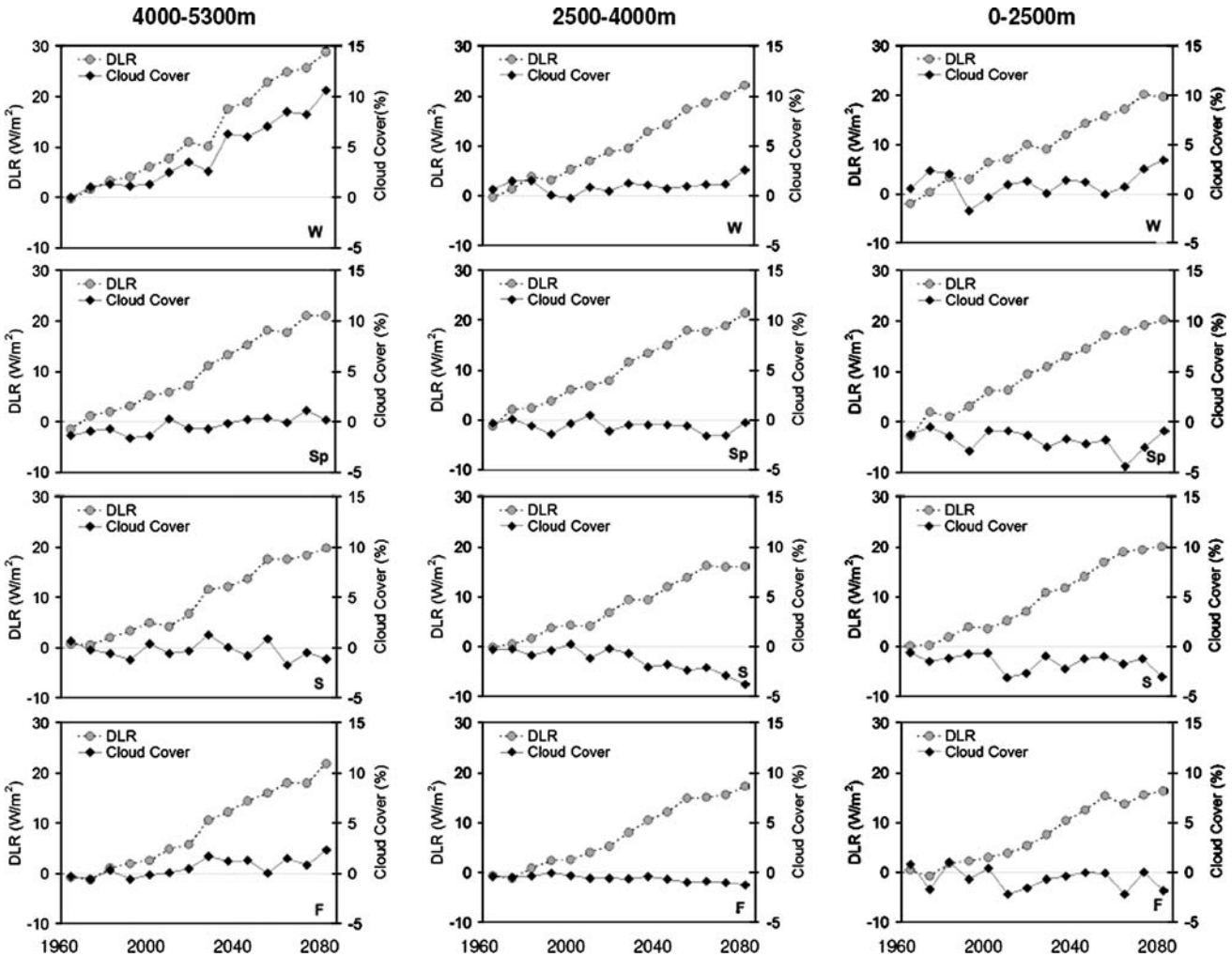


**Fig. 8** Same as Fig. 7, but for DLR (W/m$^2$) and cloud cover (%)

temperature increases are similar for both seasons (Rangwala et al. 2009). This phenomenon could be associated with changes in snow cover in the region. Xu et al. (2007) report a widespread decrease in precipitation over the plateau during the summer months between 1960 and 2000, and significant increases during spring. The latter is consistent with the increases in snow depth (Zhang et al. 2004) and cloud cover (Li et al. 2005) over the plateau during spring since the mid-1970s. Our analysis of the observations suggests precipitation increases during winter and spring, and small decreases during fall (low elevation) and summer (high elevation) (Rangwala et al. 2009). Therefore, the large increases in maximum temperature during fall relative to spring could be, in part, a result of a possible increase in snow cover extent during spring and a reduction during fall. Snow on the ground greatly reduces the absorption of solar radiation at the surface, hence suppresses the maximum temperature more than the minimum temperature (e.g. Leathers et al. 1995). Moreover, comparable increases in the minimum temperatures during spring and fall can be partly explained by similar increases in DLR.

The model simulation shows that the largest increase in maximum and minimum temperatures occurs in spring followed by winter in the latter half of the twentieth century. Fall has the smallest increases in both. This pattern is mostly explained by a large decrease in snow cover during spring (2,500–5,300 m), summer (>4,000 m) and winter (2,500–4,000 m), while fall had the smallest change in snow cover. For the twenty-first century, Fig. 9 shows that there are large decreases in snow cover (>10%) at 4,000–5,300 m during spring, fall and summer, and at 2,500–4,000 m during winter and spring. This corresponds with increases in the surface absorption of incoming solar radiation. There is little change in the snow cover at 0–2,500 m, because there is

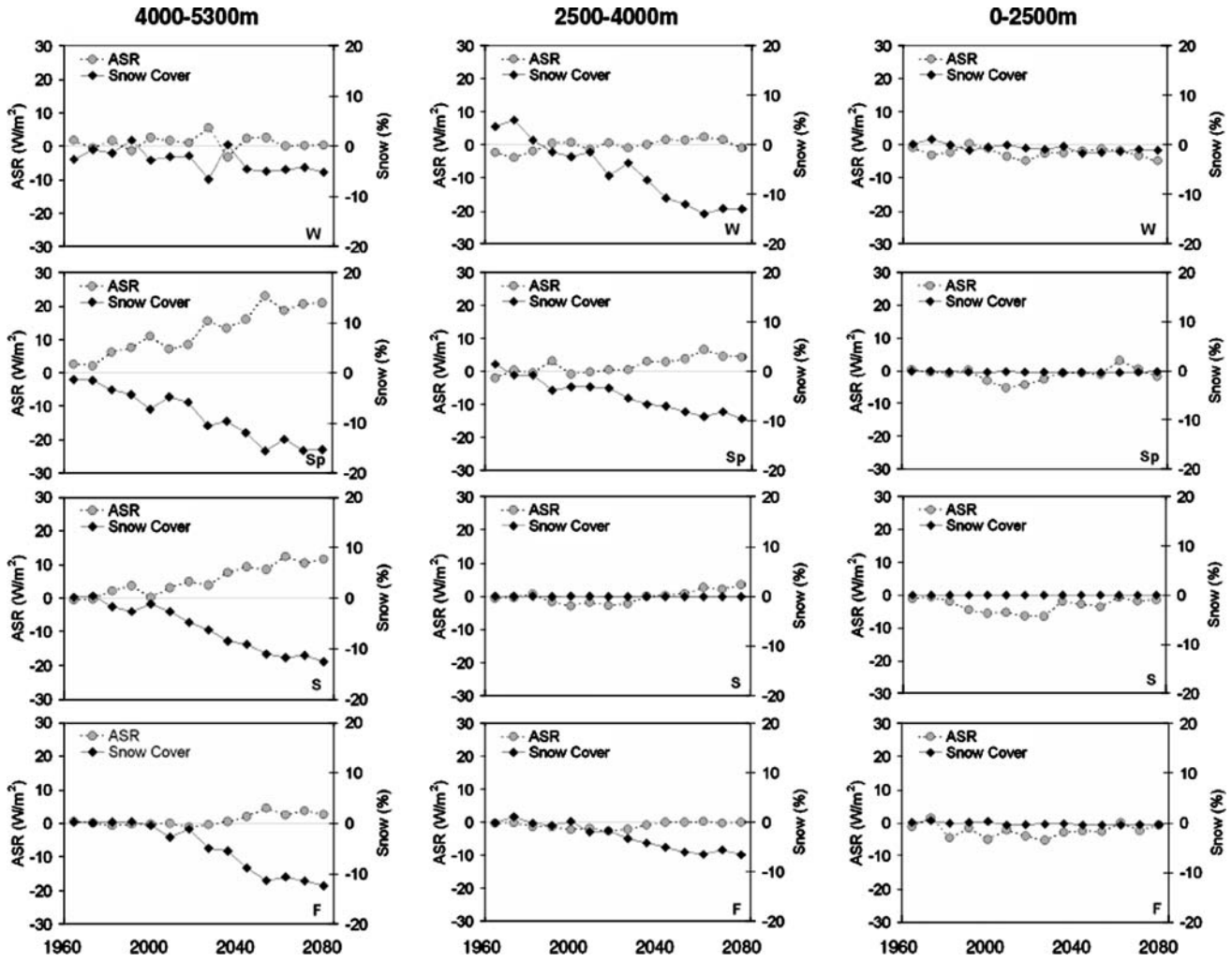


**Fig. 9** Same as Fig. 7, but for ASR (W/m$^2$) and snow cover (%)

little annual snowfall associated with these regions in the model.

As the region warms during the twenty-first century, we expect continuous reduction in snow cover during spring and summer at higher elevations as suggested by the model. This effect would accelerate the surface warming during spring and summer through the snow-albedo feedback mechanism. It is possible that the last decade of the twentieth century is already exhibiting this process when we account for a sudden increase in spring and summer temperatures at high elevations as described in Rangwala et al. (2009). Moreover, Ueno et al. (2007) suggest patchiness in snow cover on the plateau, even during winter, which may result in large surface temperature heterogeneities under strong surface insolation. Our model does not treat for patchiness in snow cover within a grid cell. Therefore, we might expect a more enhanced surface warming rate during spring and summer—periods of high surface insolation—owing to patchiness in snow cover than suggested by the model during the twenty-first century.

## 6 Effect of water vapor, snow cover and aerosols on EDW

The modeled surface temperature anomalies at elevations greater than 4,000 m tend to increase more than the anomalies at lower elevations from 1980 to 2100 (Fig. 2a). The differences in temperature anomalies associated with different elevations increase throughout the twenty-first century. Moreover, the EDW over the plateau occurs in all seasons between 1950 and 2100; however, the effect is more significant during winter and spring (Figs. 4a, 10).

For the twenty-first century, the largest increase in modeled DLR at higher elevations occurs in winter (Fig. 4b). Wintertime increases in DLR at 4,000–5,300 m

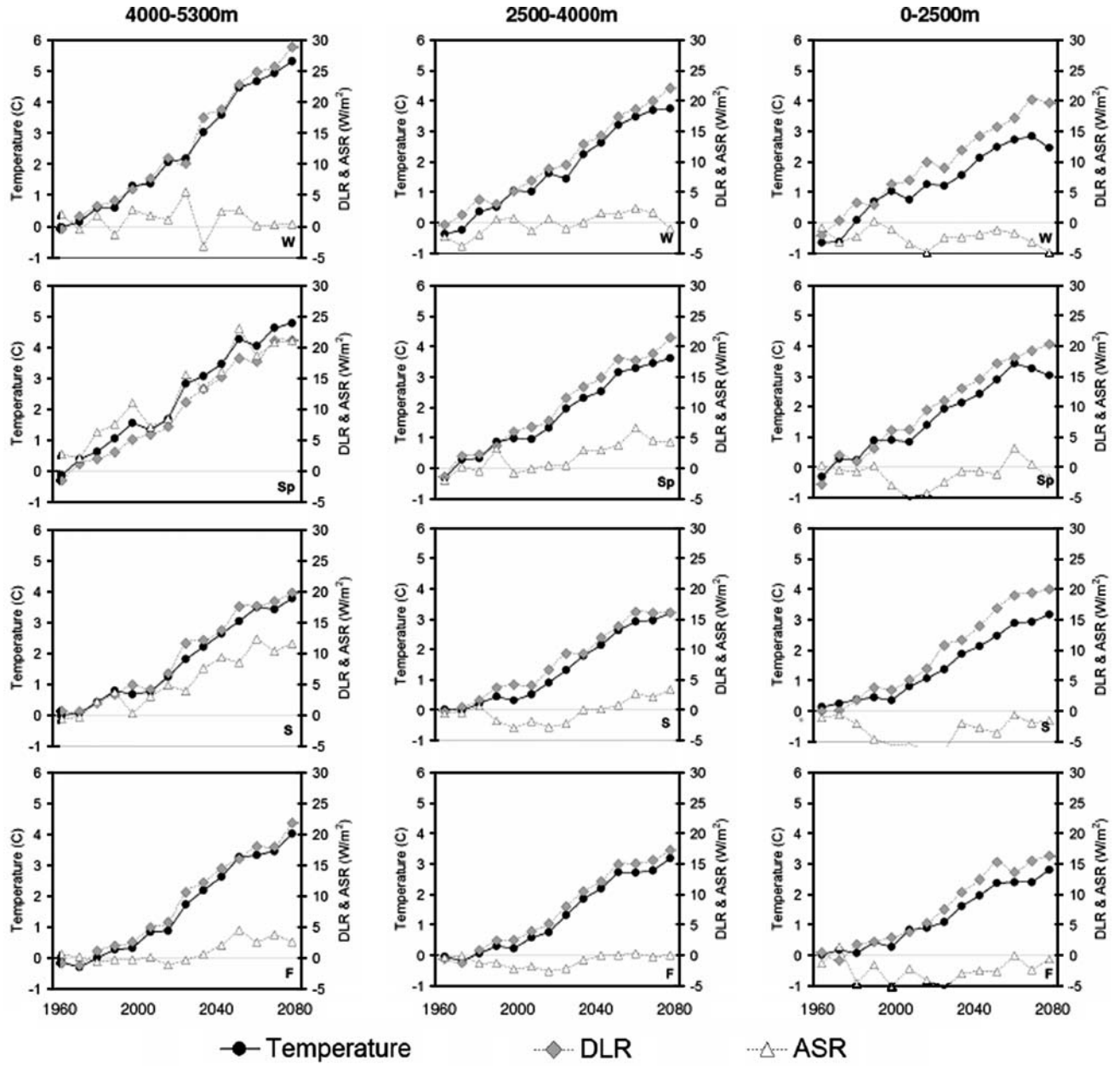


**Fig. 10** Same as Fig. 7, but for temperature (C), DLR (W/m$^2$) and ASR (W/m$^2$)

are 40% higher than the increases at 0–2,500 m. As discussed in Sect. 4, this occurs, in part, because DLR changes are highly sensitive to changes in q during winter (Fig. 6).

Higher elevations also show greater increases in ASR during the twenty-first century, but for spring and summer months (Fig. 9). During these months, ASR increases significantly more at the highest elevation than at the lower elevations despite small increasing trends in cloud cover at higher elevations (Figs. 5c, 8). The cloud cover generally decreases at the lower elevations. Figure 9 also shows that greater increases in the modeled ASR at higher elevations are primarily associated with greater decreases in snow cover at higher elevations (>2,500 m) during the 1961–2100 period, whereas the lower elevation regions have little snow cover extent in the model. In fact, lower elevation regions show decreases in ASR between 1970 and 2040 with particularly large decreases during summer. These trends appear to be associated with increases in the atmospheric sulfate burden between 1970 and 2040 (Fig. 5h). The trends in the atmospheric sulfate burden over low elevation regions are at least two times higher than at high elevation sites, both in past estimates and the projected future scenario.

For the twenty-first century, the model simulation suggests that the elevation-based differential increases in both (a) DLR—during winter, fall and spring, and (b) ASR—during spring and summer, are causing an EDW trend in the model during those periods (Fig. 10). Moreover, the model projects large increases in the atmospheric sulfate burden until the middle of the twenty-first century over the low elevation regions in the plateau, particularly during the warm season (May–September). This reduces the net solar radiation at the surface and, hence, the ASR. This factor further intensifies the EDW in the plateau by differentially decreasing the ASR in the lower elevation regions.

The observed spring and summer temperatures have risen sharply over the plateau in the last decade of the twentieth century (Rangwala et al. 2009), and we expect this trend to continue and accelerate during the twenty-first century under the influence of global greenhouse warming. A continuing increase in warming during spring and summer in the twenty-first century will increasingly influence the extent of snow cover in the high elevation regions. We, therefore, expect the EDW phenomenon to intensify over the plateau, particularly during the early half of the twenty-first century, due to elevation dependent increases in DLR and ASR as predicted by the model.

We expect very limited influence of anthropogenic land-use change on the late twentieth century climatic trends over the plateau. Deforestation on the plateau is minor due to the very small areas with forest cover. Human induced land cover change in the past decades have been mainly limited to grasslands where overgrazing is observed locally. Compared with the large area of the plateau, this human induced effect on albedo is minor because the majority of the plateau is very sparsely populated. However, the vegetation has changed considerably in some areas, possibly in response to climate change, and may have led to soil erosion and desertification. Cui et al. (2006) suggest greater warming and drying on the plateau under a widespread anthropogenic land-use change scenario.

We also analyzed trends in terrestrial evapotranspiration between 1951 and 2100 (Fig. 11). The model's evapotranspiration is a product of the potential evapotranspiration (PET) and water availability factor. The PET is proportional to the product of (a) stability based drag coefficient, (b) the surface wind speed, and (c) the difference between the saturated ground humidity and the surface air humidity. The water availability factor is based on temperature, the amount of sunlight, and wetness of the deeper rooting layers of the vegetation when the sun is up during the growing season, but simply the upper ground wetness at other times. The model shows continuous increases in evapotranspiration rates between 1951 and 2100 at 4,000–5,300 m and 2,500–4,000 m elevations, while the evapotranspiration rates at 0–2,500 m have

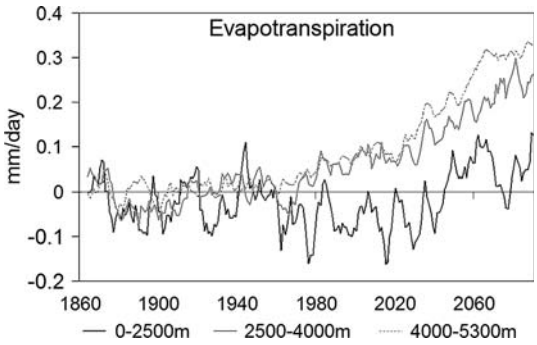


**Fig. 11** Anomalies in modeled evapotranspiration rates (mm/day) over the plateau between 1860 and 2090 at different elevations. All trends are 5-year running mean

decreased in the late twentieth and early twenty-first century. These decreases in the evapotranspiration rates at lower elevations appear to be, in part, associated with decreases in surface insolation, whereas the increases in evapotranspiration rates at higher elevations are, largely, related to the warming of the atmosphere (Table 3) and the associated increases in snow and ice melt. The relative humidity has remained relatively unchanged throughout the model simulation.

For the late twentieth century, estimates of PET on the plateau by Chen et al. (2006) and Zhang et al. (2007) have shown decreasing trends of 1.5–2.0% per decade. These decreasing trends have been linked with decreases in surface wind speed and insolation. However, estimates of actual evapotranspiration (AET) from limited sites on the plateau during the late twentieth century suggest an increasing trend of +7.0 mm/year per decade (Zhang et al. 2007). For the 1961–2000 period, the model trends in evapotranspiration rates are +6.1 (+1.2%), +11.3 (+1.3%) and +0.2 (+0.03%) mm/year per decade (% change from annual total per decade) respectively at 4,000–5,300 m, 2,500–4,000 m and 0–2,500 m. The model trends in evapotranspiration rates at higher elevations are similar to the AET trends measured by Zhang et al. (2007). They suggest that increases in stream discharge rate owing to widespread glacier retreats over the plateau may, in part, be responsible for increases in the observed AET trends.

## 7 Conclusions

In this study, we have used a global climate model to understand the mechanisms for the observed climate change reported over the Tibetan Plateau in the latter half of the twentieth century (Du et al. 2004; Liu and Chen 2000; Niu et al. 2004; Rangwala et al. 2009; Xu et al. 2007) and to examine potential climate change through the twenty-first century.

**Table 3** Correlation ($r$) of modeled evapotranspiration rates with several climate variables between 1951 and 2050

| Elevation (m) | Correlation ($r$) with evaporation rate | | | |
|---|---|---|---|---|
| | Wind speed | Soil moisture | Surface insolation | Temperature |
| 4,000–5,300 | 0.18 | −0.39 | 0.65 | 0.92 |
| 2,500–4,000 | 0.25 | −0.26 | 0.19 | 0.68 |
| 0–2,500 | −0.04 | 0.68 | −0.32 | −0.04 |

For the 1961–2000 period, we find that the model's warming trend is similar to the observed trend reported in Rangwala et al. (2009). The model simulation generates a 4°C warming between 1951 and 2100 under the SRES A1B scenario, with the largest warming rates occurring during winter and spring. The model experiment also generates an EDW trend between 1951 and 2100. This trend becomes larger in the latter half of the twenty-first century. For the 1961–1990 period, the model's EDW trend is comparable to the observed trend reported by Liu and Chen (2000). Similar to the temperature trend, there are elevation-based increases in surface vapor pressure, ASR, DLR and latent heat fluxes, and decreases in snow cover between 1951 and 2100. The atmospheric sulfate burden, which peaks around 2030 and decreases in the latter half of the twenty-first century, shows larger increases at lower elevations than at the highest elevations.

The model simulation suggests that an accelerated wintertime warming results from large increases in DLR during winter months. These increases in DLR are caused by increases in specific humidity, particularly when the specific humidity is low (Ruckstuhl et al. 2007), which occurs most prominently during winter months at higher elevations (Rangwala et al. 2009). This mechanism, therefore, tends to cause the largest net increases in DLR at higher elevations during the winter months in the model and contributes to an EDW during winter. This mechanism is also important during spring and fall, although weaker.

Another factor in the warming is the snow-albedo effect. There are large increases in ASR at higher elevation, particularly during spring and summer, which can increase the surface temperature. These increases in ASR are largely associated with decreases in snow cover. Previous modeling studies have also suggested that snow-albedo feedback is one of the primary factors in causing an EDW in the high mountain regions (Chen et al. 2003; Giorgi et al. 1997). Observed increases in precipitation (Xu et al. 2007) and snowdepth (Zhang et al. 2004) during spring suggest that snow cover over the plateau might not be significantly affected during spring in the latter half of the twentieth century. However, as the greenhouse warming continues into the twenty-first century, we expect to see an accelerated surface warming during spring and summer, particularly at higher elevations, due to a continuous reduction in the snow cover.

Moreover, there is a decreasing trend in the ASR in the low elevation region in the early half of the twenty-first century owing, in part, to large increases in the atmospheric sulfate burden relative to the high elevation sites. The net effect of changes in snow cover and atmospheric sulfate burden is to produce an elevation dependent increase in ASR during the twenty-first century.

Our analysis suggests that the Tibetan Plateau will warm during the twenty-first century under the SRES A1B scenario. This warming is likely to be more pronounced at higher elevations in the plateau due to (a) increases in DLR caused by surface humidity increases during cold seasons, (b) increases in ASR caused by decreases in the snow cover extent during spring and summer and (c) larger aerosol concentrations at lower elevations. The elevation-based changes in surface energy balance affected by changes in surface humidity, snow cover and atmospheric aerosol will also tend to produce an EDW trend over the plateau during the twenty-first century.

**Acknowledgments** We would like to thank the anonymous reviewers for their helpful comments that have significantly improved our manuscript. Partial support for JRM has been provided by Project #32103 from the NJ Agricultural Experiment Station.

## References

Boucher O, Pham M (2002) History of sulfate aerosol radiative forcings. Geophys Res Lett 29:1308. doi:10.1029/2001GL014048

Chen B, Chao WC, Liu X (2003) Enhanced climatic warming in the Tibetan Plateau due to doubling $CO_2$: a model study. Clim Dyn 20:401–413

Chen S, Liu Y, Thomas A (2006) Climatic change on the Tibetan Plateau: potential evapotranspiration trends from 1961–2000. Clim Change 76:291–319. doi:10.1007/s10584-006-9080-z

Cui X, Graf H, Langmann B, Chen W, Huang R (2006) Climate impacts of anthropogenic land use changes on the Tibetan Plateau. Glob Planet Change 54:33–56. doi:10.1016/j.gloplacha.2005.07.006

Du M, Kawashima S, Yonemura S, Zhang X, Chen S (2004) Mutual influence between human activities and climate change in the Tibetan Plateau during recent years. Glob Planet Change 41:241–249. doi:10.1016/j.gloplacha.2004.01.010

Duan A, Wu G (2006) Change of cloud amount and the climate warming on the Tibetan Plateau. Geophys Res Lett 33:L22704. doi:10.1029/2006GL027946

Giorgi F, Hurrell J, Marinucci M, Beniston M (1997) Elevation dependency of the surface climate change signal: a model study.

J Clim 10:288–296. doi:10.1175/1520-0442(1997)010<0288:EDOTSC>2.0.CO;2

Houghton J, Ding Y, Griggs D, Noguer M, van der Linden P, Dai X, Maskell K, Johnson C (2001) Climate change 2001: the scientific basis. Contribution of Working Group I to the Third Assessment Report of the Intergovernmental Panel on Climate Change. Cambridge University Press, Cambridge

Leathers D, Ellis A, Robinson D (1995) Characteristics of temperature depressions associated with snow cover across the northeast United States. J Appl Meteorol 34:381–390

Levitus S, Burgett R, Boyer TP (1994) World ocean atlas 1994. Vol. 3. Salinity, NOAA Atlas NESDIS 3, p 99

Li J, Yu R, Zhou T, Wang B (2005) Why is there an early spring cooling shift downstream of the Tibetan Plateau? J Clim 18:4660–4668. doi:10.1175/JCLI3568.1

Liu X, Chen B (2000) Climatic warming in the Tibetan Plateau during recent decades. Int J Climatol 20:1729–1742. doi:10.1002/1097-0088(20001130)20:14<1729::AID-JOC556>3.0.CO;2-Y

Liu B, Xu M, Henderson M, Qi Y, Li Y (2004) Taking China's temperature: daily range, warming trends, and regional variations, 1955–2000. J Clim 17:4453–4462. doi:10.1175/3230.1

New M, Hulme M, Jones P (1999) Representing twentieth-century space–time climate variability. Part I: Development of a 1961–90 mean monthly terrestrial climatology. J Clim 12:829–856

Niu T, Chen L, Zhou Z (2004) The characteristics of climate change over the Tibetan Plateau in the last 40 years and the detection of climatic jumps. Adv Atmos Sci 21:193–203. doi:10.1007/BF02915705

Pham M, Boucher O, Hauglustaine D (2005) Changes in atmospheric sulfur burdens and concentrations and resulting radiative forcings under IPCC SRES emission scenarios for 1990–2100. J Geophys Res 110:D06112. doi:10.029/2004JD005125

Rangwala I, Miller J, Russell G, Xu M (2006) Analysis of global climate model experiments to elucidate past and future changes in surface insolation and warming in China. Geophys Res Lett 33:L20709. doi:10.1029/2006GL027778

Rangwala I, Miller JR, Xu M (2009) Warming in the Tibetan Plateau: possible influences of the changes in surface water vapor. Geophys Res Lett 36:L06703. doi:10.1029/2009GL037245

Ruckstuhl C, Philipona R, Morland J, Ohmura A (2007) Observed relationship between surface specific humidity, integrated water vapor, and longwave downward radiation at different altitudes. J Geophys Res 112:L19809. doi:10.1029/2005GL023624

Russell G, Miller J, Rind D (1995) A coupled atmosphere-ocean model for transient climate change studies. Atmos Ocean 33:683–730

Ueno K, Tanaka K, Tsutsui H, Li M (2007) Snow cover conditions in the Tibetan Plateau observed during the winter of 2003/2004. Arct Antarct Alp Res 39:152–164. doi:10.1657/1523-0430(2007)39[152:SCCITT]2.0.CO;2

Xu M, Chang C, Fu C, Qi Y, Robock A, Robinson D, Zhang H (2006) Steady decline of East Asian monsoon winds, 1969–2000: evidence from direct ground measurements of wind speed. J Geophys Res 111:D24111. doi:10.1029/2006JD007337

Xu Z, Gong T, Li J (2007) Decadal trend of climate in the Tibetan Plateau-regional temperature and precipitation. Hydrological Processes. doi: 10.1002/hyp.6892. ISSN: 1099–1085

You Q, Kang S, Wu Y, Yan Y (2007) Climate change over the Yarlung Zangbo river basin during 1961–2005. J Geogr Sci 17:409–420. doi:10.1007/s11442-007-0409-y

You Q, Kang S, Pepin N, Yan Y (2008) Relationship between trends in temperature extremes and elevation in the eastern and central Tibetan Plateau, 1961–2005. Geophys Res Lett 35:L04704. doi:10.1029/2007GL032669

Zhang Y, Li T, Wang B (2004) Decadal change of the spring snow depth over the Tibetan Plateau: the associated circulation and influence on the East Asian summer monsoon. J Clim 17:2780–2793. doi:10.1175/1520-0442(2004)017<2780:DCOTSS>2.0.CO;2

Zhang Y, Liu C, Tang Y, Yang Y (2007) Trends in pan evaporation and reference and actual evapotranspiration across the Tibetan Plateau. J Geophys Res 112:D12110. doi:10.1029/2006JD008161